Electronic Supplementary Material (ESI) for Catalysis Science & Technology.
This journal is © The Royal Society of Chemistry 2019

Electronic Supplementary Information

In situ synthesis of FeP decorated Ti-Fe_2O_3: An effective strategy to improve interfacial charge transfer in photoelectrochemical water oxidation reaction

Qijing Bu,[a] Shuo Li,[b] Qiannan Wu,[a] Yanhong Lin,[a] Dejun Wang,[a] Xiaoxin Zou,[c] and Tengfeng Xie*, [a]

[a] College of Chemistry, Jilin University, Changchun 130012, P. R. China

[b] Liaoning Key Laboratory for Green Synthesis and Preparative Chemistry of Advanced Materials, College of Chemistry, Liaoning University, Shenyang 110036, P. R. China

[c] State Key Laboratory of Inorganic Synthesis and Preparative Chemistry, College of Chemistry, Jilin University, Changchun 130012, P. R. China

E-mail: xietf@jlu.edu.cn

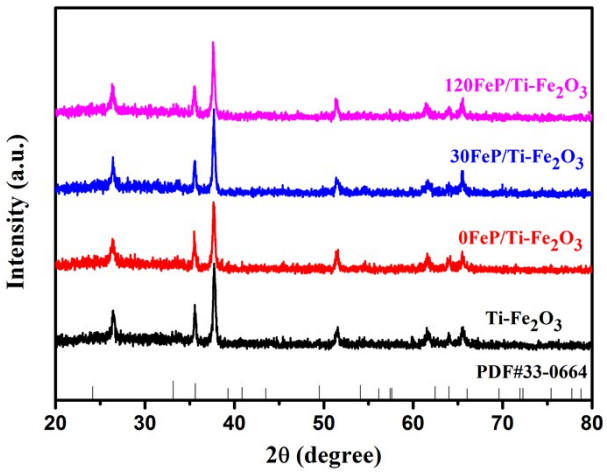

Figure S1 XRD patterns of Ti-Fe_2O_3 and FeP/Ti-Fe_2O_3.

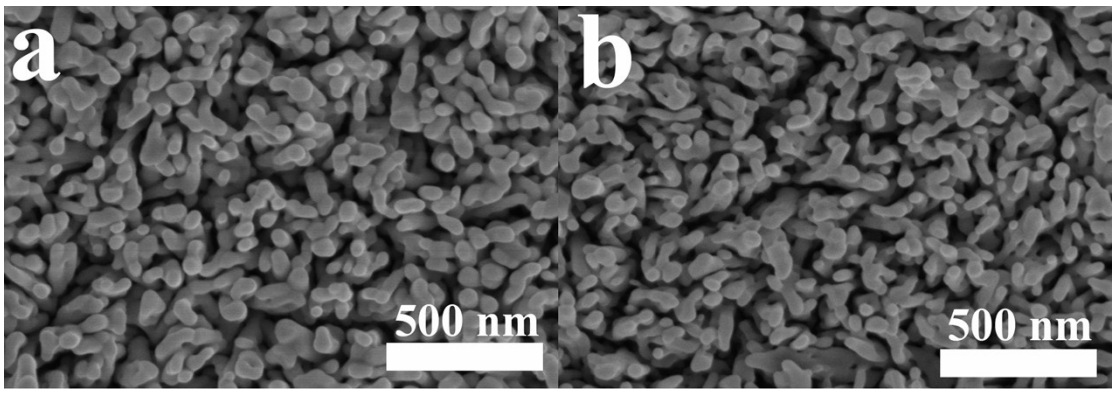

Figure S2 Top-view FE-SEM images of Ti-Fe_2O_3 (a) and 0FeP/Ti-Fe_2O_3 (b).

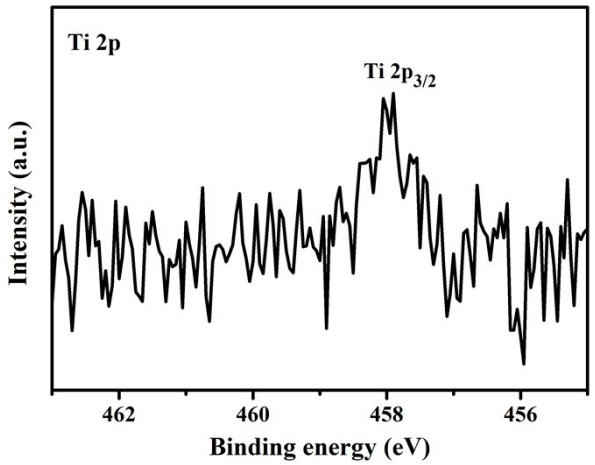

Figure S3 XPS spectrum of Ti 2p for Ti-Fe_2O_3.

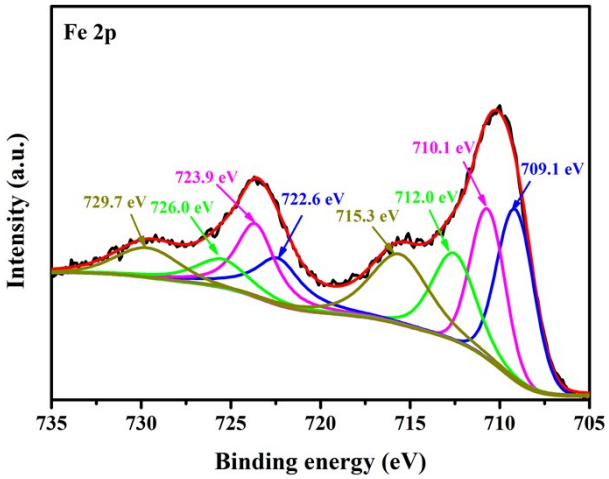

Figure S4 XPS spectrum of Fe 2p for 0FeP/Ti-Fe_2O_3.

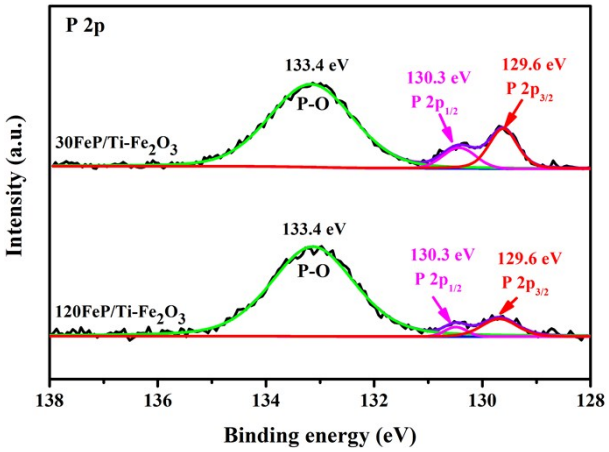

Figure S5 XPS spectra of P 2p for 30FeP/Ti-Fe_2O_3 and 120FeP/Ti-Fe_2O_3.

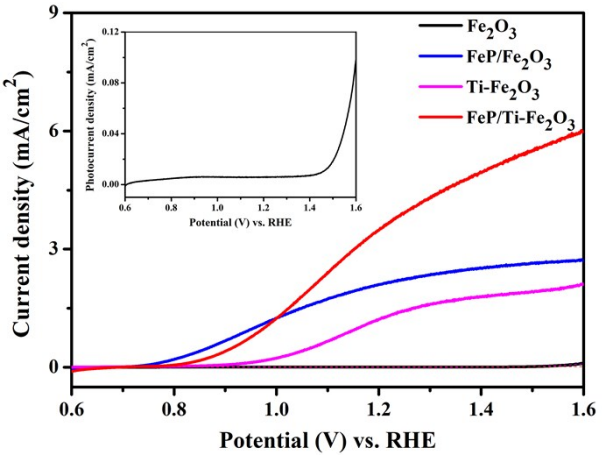

Figure S6 Current-potential curves of Fe_2O_3, 0FeP/Fe_2O_3, Ti-Fe_2O_3 and 0FeP/Ti-Fe_2O_3 in dark and under AM 1.5 G illumination in 1 M KOH electrolyte solution. The inset shows the photocurrent density-potential curve of Fe_2O_3.

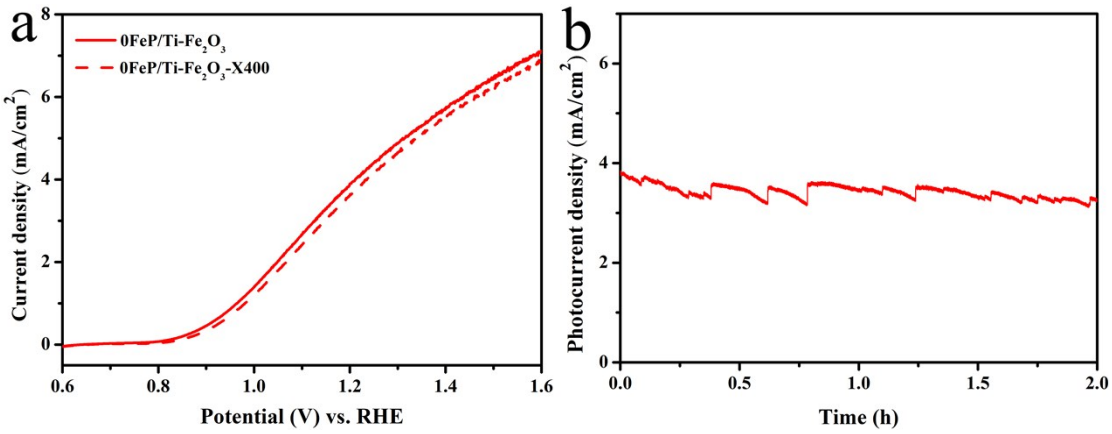

Figure S7 (a) Photocurrent-potential curves of 0FeP/Ti-Fe_2O_3 in 1 M KOH with or without one drop of Triton X-400. (b) Photostability measurement of 0FeP/Ti-Fe_2O_3 at 1.23 V vs. RHE in 1 M KOH with one drop of Triton X-400.

It is noted that Triton X-400 is used to clear the generated bubbles during the photostability test.

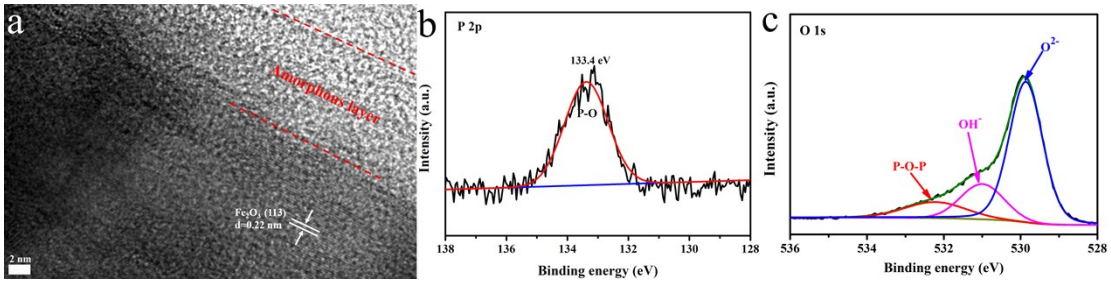

Figure S8 HRTEM image (a), XPS spectra of P 2p (b) and O 1s (c) for 0FeP/Ti-Fe_2O_3 after the photostability measurement.

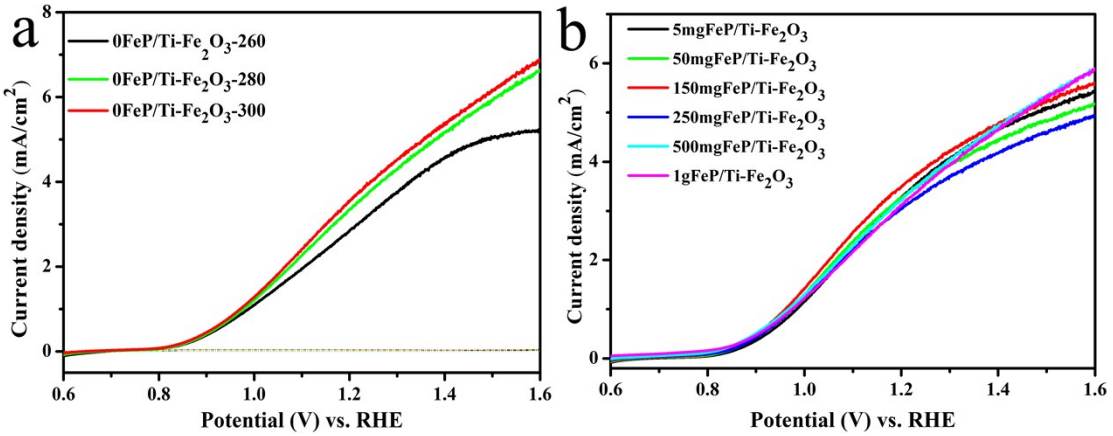

Figure S9 Photocurrent-potential curves of FeP/Ti-Fe_2O_3 by changing the

phosphidation temperature (a) and the amount of NaH_2PO_2 (b).

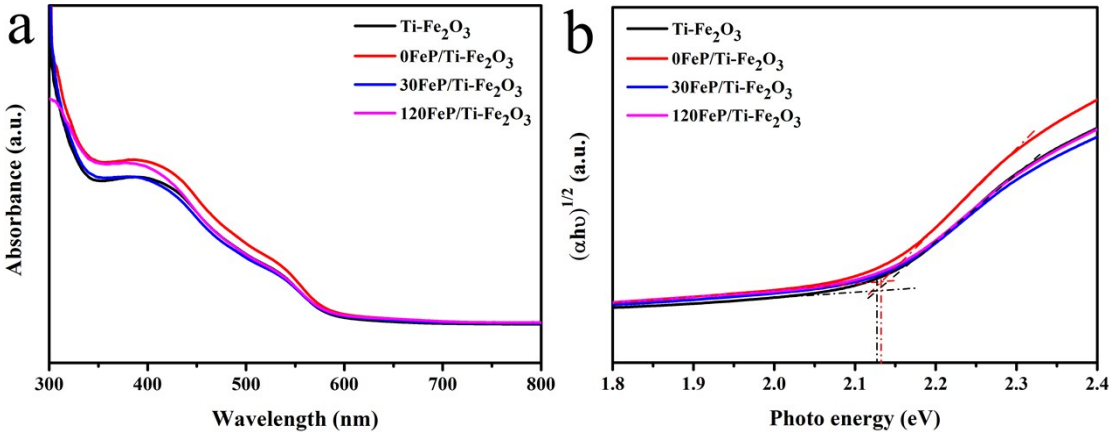

Figure S10 UV-vis absorption spectra (a) and the corresponding Tauc's plots (b) of Ti-Fe_2O_3 and FeP/Ti-Fe_2O_3.

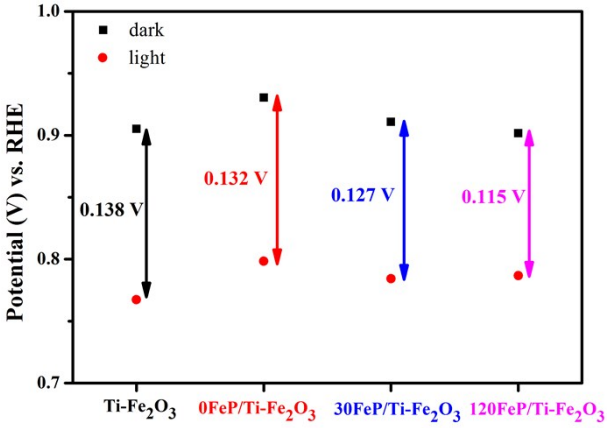

Figure S11 Open-circuit potentials of Ti-Fe_2O_3 and FeP/Ti-Fe_2O_3 in dark and under AM 1.5 G illumination.

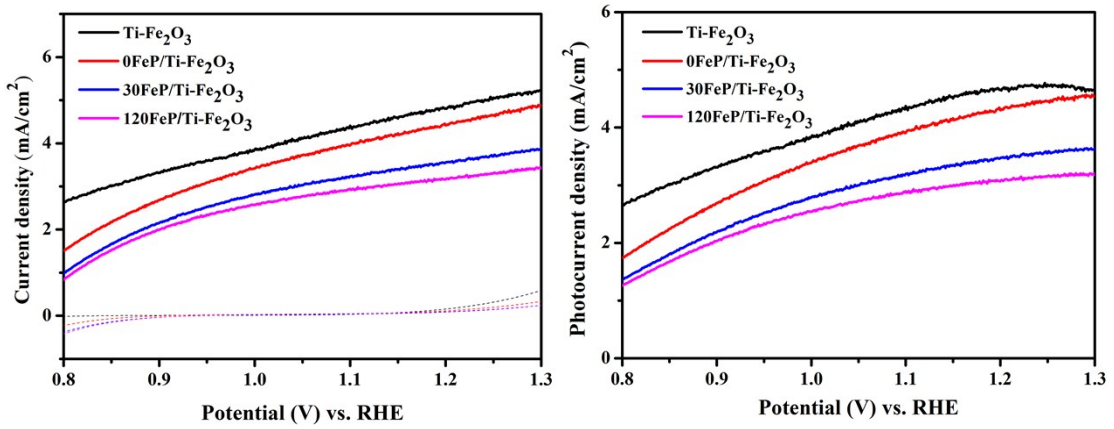

Figure S12 Current-potential curves (a) and Photocurrent-potential curves (b) of Ti-

Fe_2O_3 and FeP/Ti-Fe_2O_3 in dark and under AM 1.5 G illumination in 1 M KOH added 0.5 M H_2O_2.

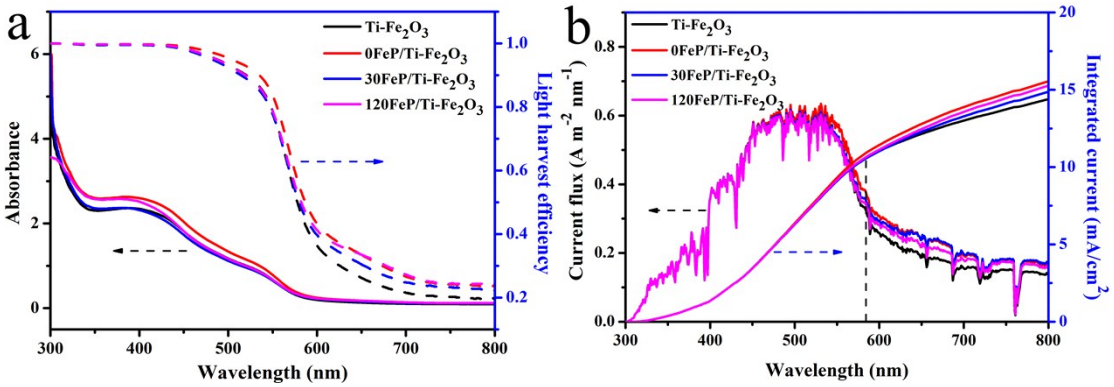

Figure 13 (a) The absorption (solid line) and light harvest efficiency (dash line) of Ti-Fe_2O_3 and FeP/Ti-Fe_2O_3. (b) The calculated current density flux and integrated current density (J_{abs}) of Ti-Fe_2O_3 and FeP/Ti-Fe_2O_3.

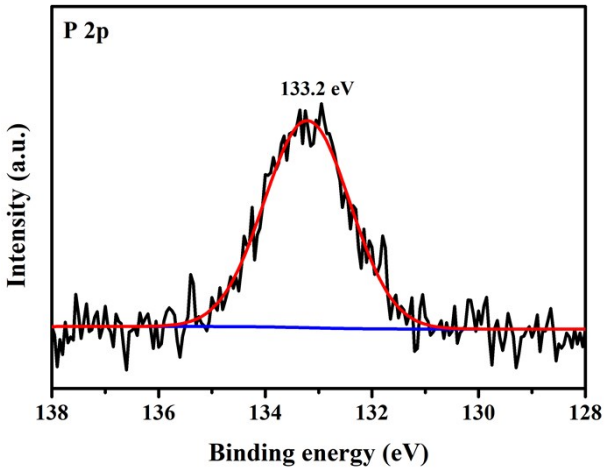

Figure 14 XPS spectrum of P 2p for etched 0FeP/Ti-Fe_2O_3 using argon sputtering.

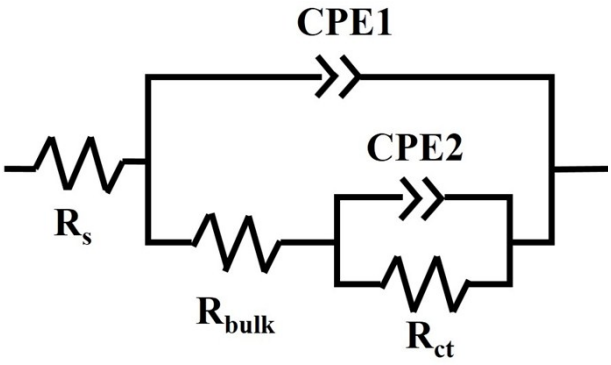

Figure S15 The equivalent circuit model for fitting Nyquist plots of photoanodes.

Table S1 Comparison of the photocurrent density of Fe_2O_3 in literature with our result under AM 1.5 G illumination

Composite	Photocurrent density at 1.23V vs. RHE	Electrolyte	Ref
Fe_xS|Vo|Fe_2O_3	2.30 mA/cm^2	1 M NaOH	[1]
CoPi/Pt-Fe_2O_3	4.32 mA/cm^2	1M NaOH	[2]
Ti:Fe_2O_3@GCNN-CQDs	3.38 mA/cm^2	1 M KOH	[3]
NiO/P-α-Fe_2O_3	2.08 mA/cm^2	1 M KOH	[4]
Fe_2O_3/C_3N_4/CoO_x	1.50 mA/cm^2	1 M NaOH	[5]
Fe_2TiO_5/Fe_2O_3/Pt	1.0 mA/cm^2	1 M KOH	[6]
ITO/Fe_2O_3/Fe_2TiO_5/FeNiOOH	2.2mA/cm^2	1 M NaOH	[7]
Fe_2O_3/FeB/CoPi	1.9 mA/cm^2	1 M NaOH	[8]
Ti-Fe2O3-FeOOH	2.31 mA/cm^2	1 M KOH	[9]
C/Co_3O_4-Fe_2O_3	1.48 mA/cm^2	1 M NaOH	[10]
Ti-Fe_2O_3/$Ni(OH)_2$/IrO_2	2.2 mA/cm^2	1 M NaOH	[11]
CoPi/Ag/Fe_2O_3	4.68 mA/cm^2	1 M NaOH	[12]
FeOOH/α-Fe_2O_3 NF/Pt	2.0 mA/cm^2	1 M KOH	[13]
Fe2O3/Fe2TiO5/SnOx	1.0 mA/cm^2	1 M KOH	[14]
FeP/Ti-Fe_2O_3	3.9 mA/cm^2	1 M KOH	In this

			work

Table S2 The atomic ratio of Fe and P for 0FeP/Ti-Fe_2O_3, 30FeP/Ti-Fe_2O_3 and 120FeP/Ti-Fe_2O_3

sample	0FeP/Ti-Fe_2O_3	30FeP/Ti-Fe_2O_3	120FeP/Ti-Fe_2O_3
Fe:P	13.04	9.22	6.04

Table S3 The fitted results of Nyquist plots for Ti-Fe_2O_3 and FeP/Ti-Fe_2O_3.

Photoanode	R_{bulk} [Ω]	CPE1 [10^{-4}Fcm^{-2}]	R_{ct} [Ω]	CPE2 [10^{-5}Fcm^{-2}]
Ti-Fe_2O_3	137.8	2.775	1650	4.483
0FeP/Ti-Fe_2O_3	94.76	3.499	337.6	3.562
30FeP/Ti-Fe_2O_3	206.4	2.044	536.9	2.071
120FeP/Ti-Fe_2O_3	185.4	2.336	639.9	2.093

REFERENCE

1. A. Liao, R. Chen, F. Fan, L. Xiao, H. He, C. Zhang, A. M. Asiri, Y. Zhou, C. Li and Z. Zou, *Chem. Commun.*, 2018, **54**, 13817-13820.

2. J. Y. Kim, G. Magesh, D. H. Youn, J.-W. Jang, J. Kubota, K. Domen and J. S. Lee, *Sci. Rep.*, 2013, **3**, 2681.

3. S.-S. Yi, J.-M. Yan and Q. Jiang, *J. Mater. Chem. A*, 2018, **6**, 9839-9845.

4. F. Li, J. Li, J. Zhang, L. Gao, X. Long, Y. Hu, S. Li, J. Jin and J. Ma, *ChemSusChem*, 2018, **11**, 2156-2164.

5. Z. Mei, Y. Li, X. Yang, W. Ren, S. Tong, N. Zhang, W. Zhao, Y. Lin and F. Pan, *Catal. Sci. Technol.*, 2018, **8**, 3144-3150.

6. L. Wang, N. Nhat Truong, X. Huang, P. Schmuki and Y. Bi, *Adv. Funct. Mater.*, 2017, **27,** 1703527.

7. P. Tang, H. Xie, C. Ros, L. Han, M. Biset-Peiro, Y. He, W. Kramer, A. P. Rodriguez, E. Saucedo, J. R. Galan-Mascaros, T. Andreu, J. R. Morante and J. Arbiol, *Energy Environ. Sci.*, 2017, **10**, 2124-2136.

8. A. Liao, H. He, Z. Fan, G. Xu, L. Li, J. Chen, Q. Han, X. Chen, Y. Zhou and Z. Zou, *J. Catal.*, 2017, **352**, 113-119.

9. Y. Yuan, J. Gu, K.-H. Ye, Z. Chai, X. Yu, X. Chen, C. Zhao, Y. Zhang and W. Mai, *ACS App. Mater. Interfaces*, 2016, **8**, 16071-16077.

10. P. Zhang, T. Wang, X. Chang, L. Zhang and J. Gong, *Angew. Chem. Int. Ed.*, 2016, **55**, 5851-5855.

11. Z. Wang, G. Liu, C. Ding, Z. Chen, F. Zhang, J. Shi and C. Li, *J. Phys. Chem. C*, 2015, **119**, 19607-19612.

12. P. Peerakiatkhajohn, J.-H. Yun, H. Chen, M. Lyu, T. Butburee and L. Wang, *Adv. Mater.*, 2016, **28**, 6405-6410.

13. L. Wang, Y. Yang, Y. Zhang, Q. Rui, B. Zhang, Z. Shen and Y. Bi, *J. Mater. Chem. A*, 2017, **5**, 17056-17063.

14. L. Wang, N. Nhat Truong and P. Schmuki, *ChemSusChem*, 2016, **9**, 2048-2053.